Earth and Planetary Science Letters 373 (2013) 150–159

Contents lists available at SciVerse ScienceDirect

Earth and Planetary Science Letters

journal homepage: www.elsevier.com/locate/epsl

Petrogenetic association of the oldest lunar basalts: Combined Rb–Sr isotopic and trace element constraints

Hejiu Hui [a,*], Clive R. Neal [a], Chi-Yu Shih [b], Laurence E. Nyquist [c]

[a] Department of Civil & Environmental Engineering & Earth Sciences, University of Notre Dame, Notre Dame, IN 46556, USA
[b] Jacobs Technology, ESCG, Mail Code JE23, Houston, TX 77058, USA
[c] ARES, NASA-Johnson Space Center, Mail Code KR, Houston, TX 77058, USA

ARTICLE INFO

Article history:
Received 9 April 2012
Received in revised form
11 April 2013
Accepted 23 April 2013
Editor: T. Elliot
Available online 25 May 2013

Keywords:
Apollo 14
high-Al basalt
Rb–Sr isotopic system
radiometric age
incompatible trace element
mixing

ABSTRACT

We report a new radiometric Rb–Sr age determination of 4.03 ± 0.04 Ga for high-Al basaltic clast 14321,1353, which is a Group B Apollo 14 high-Al basalt based on its whole-rock incompatible-trace-element chemistry. In addition, available literature Rb–Sr isotope data for Apollo 14 high-Al basalts were reprocessed using the same decay constant and data reduction protocol as used for sample 14321,1353. The Rb–Sr isotopic ages of high-Al basalts range from 4.31 ± 0.17 to 3.93 ± 0.06 Ga. The trace element and Rb–Sr isotopic compositions of high-Al basalts are distinct from those of Apollo 14 aluminous impact melts that crystallized at 3.86 ± 0.01 Ga. The Rb–Sr isotope systematics, coupled with incompatible-trace-element data are consistent with the parental melts of Apollo 14 high-Al basalts being derived from sources consisting of primitive crystallization products of the lunar magma ocean that were variably metasomatized by late-stage KREEP-rich fluids. Our new Rb–Sr isotopic age for 14321,1353 suggests that the KREEP metasomatism must occur in the lunar mantle no later than 4.03 ± 0.04 Ga. Collectively, the Apollo 14 high-Al basalts represent the earliest known volcanic products from the Moon and place a time constraint on the formation of the high-Al basalt source through the crystallization of the lunar magma ocean.

1. Introduction

Apollo 14 pristine high-Al basalts (hereafter, high-Al basalts) represent the oldest volcanic materials returned from the Moon (e.g., Dasch et al., 1987; Nyquist and Shih, 1992) and are named due to relative enrichment of Al_2O_3 (>11 wt%) compared to most of the other mare basalts (7–11 wt%) (Fig. 1a; e.g., Ridley, 1975; Neal and Taylor, 1992). Some basalts returned by Apollo 12 and Luna 16 missions contain comparable Al_2O_3 content (i.e., >11 wt%), but are characterized by younger ages (Fig. 1a). On the basis of whole-rock instrumental-neutron-activation (INA) data, the high-Al basalts were originally classified into five compositional types (Dickinson et al., 1985). Shervais et al. (1985) also proposed a subdivision of Apollo 14 basalts into five different types that was not fully comparable to the designations proposed by Dickinson et al. (1985), as it included other "low-Al" basaltic melts (such as olivine vitrophyres and tridymite ferrobasalt). Using whole-rock incompatible-trace-element (ITE) ratios, the high-Al basalts have been re-defined into three groups plus 14072: Groups A–C corresponding to Groups 4 and 5, Groups 1 and 2, and Group 3 basalts in Dickinson et al. (1985), (Fig. 1b; Neal and Kramer, 2006). Literature Rb–Sr isotopic data show that eruption episodes for the high-Al basalts span from ~4.3 Ga to ~3.95 Ga (Fig. 1c; e.g., Papanastassiou and Wasserburg, 1971; Compston et al., 1971a, 1972; de Laeter et al., 1973; Mark et al., 1973, 1974, 1975; Nyquist, 1977; Dasch et al., 1987, 1991). Therefore, the high-Al basalts could record lunar mantle evolution between the time of lunar crust formation (~4.4 Ga) and the main basin-filling mare volcanism (<3.85 Ga) (Fig. 1a; e.g., Borg et al., 2011; Shearer et al., 2006).

Although both have a "high Al" signature, the high-Al basalts are geochemically and texturally distinct relative to the Apollo 14 aluminous impact melts (hereafter, impact melts) in terms of their siderophile element abundances, ITE ratios, and crystal size distributions (CSDs) (e.g., Warren et al., 1997; Neal and Kramer, 2006; Hui et al., 2011; Neal et al., 2011). The characteristic high-Al signature for the high-Al basalts originated from their mantle source, whereas that of the impact melts was inherited from the melting of crustal materials during meteoroid/asteroid impact (Neal and Kramer, 2006; Hui et al., 2011).

Most of the high-Al basalts were found as clasts (1–3 cm in diameter typically) in breccia 14321, which also produced a collection of other important rock clasts, such as troctolite (,1154; Lindstrom et al., 1984), dunite (,1141; Lindstrom et al., 1984), alkali anorthosite (,1060; Warren et al., 1983a), granite (,1027; Warren

* Corresponding author. Tel.: +1 574 631 2613.
E-mail addresses: hhui@nd.edu, hui.hejiu@gmail.com (H. Hui).

0012-821X/$ - see front matter © 2013 Elsevier B.V. All rights reserved.
http://dx.doi.org/10.1016/j.epsl.2013.04.034

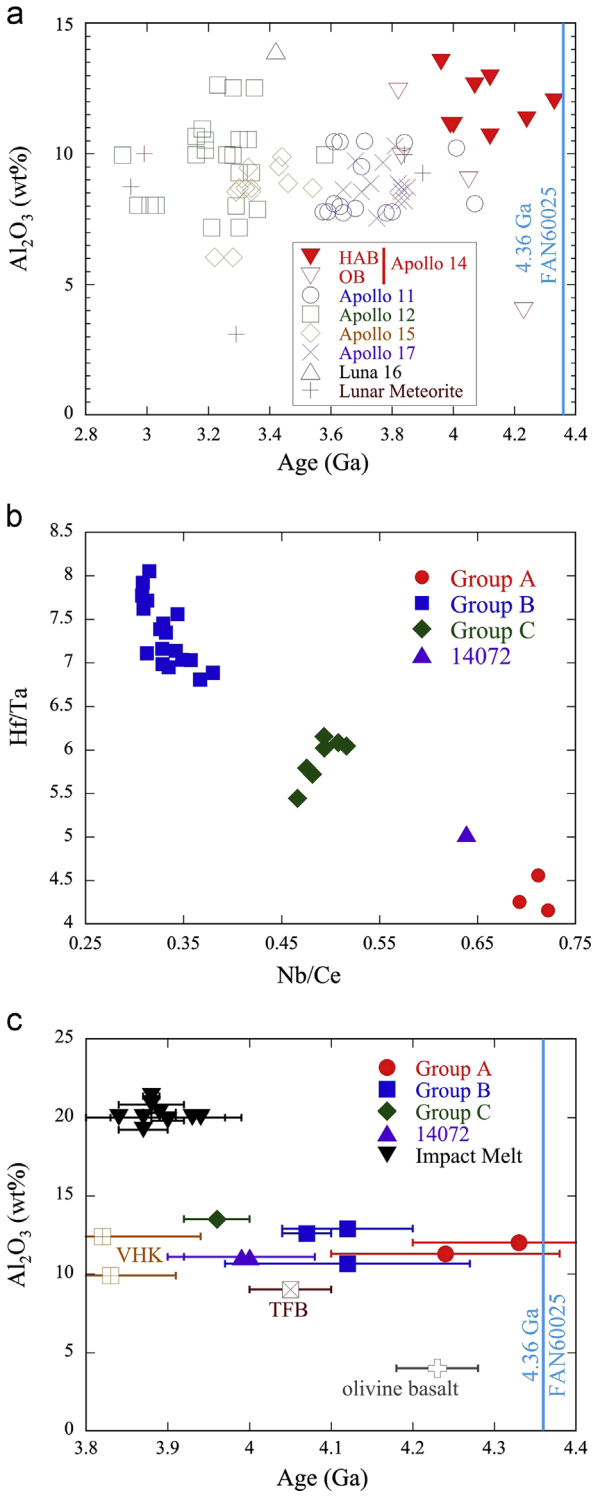

Fig. 1. (a) Comparison of Rb–Sr isochron age and whole-rock Al_2O_3 concentration between the high-Al basalts (HAB) and other mare basalts, including basalts other than high-Al basalts (OB) returned from the Apollo 14 mission. (b) Whole-rock ITE ratios (Neal and Kramer, 2006) show that the high-Al basalts can be divided into three groups plus basalt 14072. (c) Rb–Sr isochron age plotted against whole-rock Al_2O_3 concentration for Apollo 14 basaltic melts, including high-Al basalts (Groups A–C, plus basalt 14072), impact melts, very-high-potassium (VHK) basalts, olivine basalt, and tridymite ferrobasalt (TFB). Note that olivine basalt and TFB do not have high-Al signature and they are also different from Mg Suite. The 4.36-Ga age of ferroan anorthosite (FAN) 60025 (Borg et al., 2011) is plotted as reference for the younger age limit for the formation of the lunar feldspathic crust. Whole-rock ITE data in Fig. 1b are from Neal and Kramer (2006). All the age and Al_2O_3 content data are from the literature listed in Electronic Appendix.

et al., 1983b) and a more evolved tridymite ferrobasalt (,1383; Shervais et al., 1985). Therefore, the samples are distinct although all their sample numbers start with 14321 due to the fact that they are clasts derived from the same polymict breccia. The short-range unmixing model suggests that the observed variation of trace-element concentrations in centimeter-sized mare basalts could have resulted from the heterogeneity within samples that are actually homogenous on a larger scale (e.g., Lindstrom and Haskin, 1978). However, the distinct ITE ratios for the different basalt groups (Neal and Kramer, 2006), as well as trace-element abundances within olivine and plagioclase (that support crystallization from different magma types; Hagerty et al., 2005; Hui et al., 2011), show that the whole-rock analyses of high-Al basaltic clasts are representative, and the compositional spread of the high-Al basalt suite is not the result of short-range unmixing (e.g., Lindstrom and Haskin, 1978). Besides the basaltic clasts in breccia 14321, the high-Al basalts also include rock samples 14053 and 14072, which are the only two hand-specimen-sized pristine basalts returned by Apollo 14 mission. Although basalts 14053 and 14072 were considered paired (i.e., two broken pieces of the same original single rock; Swann et al., 1977) and resemble each other in terms of petrography and mineralogy (e.g., Taylor et al., 2004), they have distinctly different whole-rock ITE ratios (Fig. 1b), and consequently basalt 14053 has been classified into Group C while 14072 is an ungrouped basalt (e.g., Neal and Kramer, 2006; Hui et al., 2011), possibly representing a new compositional high-Al basalt group.

Producing the observed range of high-Al basalt compositions through variable degrees of partial melting from a single source region was shown to be impossible (e.g., Dickinson et al., 1985; Shervais et al., 1985; Dasch et al., 1987; Hagerty et al., 2005). Based on whole-rock data, it was concluded that the different high-Al basalt types could have formed by partial melting of magma ocean cumulates, but separate source regions were required (Shervais et al., 1985). Neal et al. (1988, 1989) concluded that the high-Al basalts had a continuum of compositions that was generated by assimilation of a KREEP (K, REE and P rich) component by a high-Al parental magma that was undergoing fractional crystallization (an AFC process). However, this interpretation is not consistent with the three (at least) separate volcanic episodes based on existing Rb–Sr age data (e.g., Papanastassiou and Wasserburg, 1971; Dasch et al., 1987, 1991). Cyclical assimilation of KREEP by a LREE-depleted high-Al basaltic magma was proposed to reconcile this dichotomy (Neal and Taylor, 1990). Hagerty et al. (2005) reported trace-element data of individual olivine and plagioclase crystals from the high-Al basalts, and demonstrated that variable amounts of a KREEP component were added to the basalts by either assimilation, mixing into mantle sources, or impact melting (their data could not distinguish between these three processes). Moreover, a single-stage AFC process could not explain the data reported by Hagerty et al. (2005) unless an excessively large mass of KREEP was added into the parental magma before olivine crystallization (i.e., r=mass assimilated/mass crystallized=0.95). Neal and Kramer (2006) proposed at least three magmatic events were required to generate the high-Al basalts, with their Group A basalts (the oldest) evolving through closed system fractional crystallization, but Groups B and C basalts experiencing an AFC process with a KREEP–granite mixed assimilant. A combined study based on CSDs and ITE abundances of plagioclase indicates that all three groups of high-Al basalts experienced different degrees of AFC with a mixed KREEP–granite assimilant on the lunar surface (r=0.2–0.5; Hui et al., 2011). The "mixed" assimilant is reasonable given the association of KREEP and granite (Neal and Taylor, 1989) as documented in lunar samples, such as 15405 (Ryder, 1976).

Although the high-Al basalts have been separated into three different groups plus 14072 on the basis of whole-rock ITE ratios (Fig. 1b; Neal and Kramer, 2006), a distinct eruption age for a given

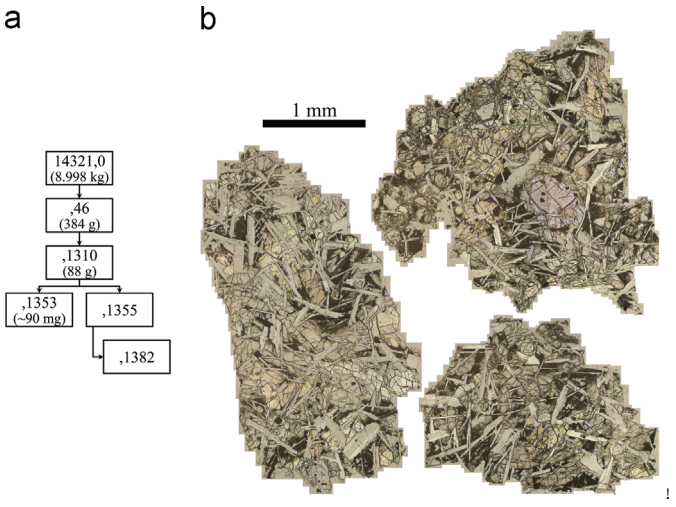

Fig. 2. (a) Genealogy of high-Al basaltic clast 14321,1353 (thin section ,1355 and ,1382). (b) Plane-polarized photomicrograph of thin section 14321,1382, indicating that no impact melt veins are present in this clast.

group based on available literature Rb–Sr geochronological results is not as clear (Fig. 1c). Uncertainties associated with the age determinations for basalt crystallization in some early studies are large (Fig. 1c); consequently, distinct eruption events producing each basalt group are not evident as isochron ages are not statistically different. However, these literature data may not be consistent with each other in part because of the use of different ^{87}Rb decay constants (e.g., Aldrich et al., 1956; Begemann et al., 2001, and references therein) and different methods used to calculate isochrons. Of note, some of the previous studies did not report the value of the ^{87}Rb decay constant that was used in their isochron calculations (e.g., Mark et al., 1975).

This paper reports new Rb–Sr isotopic data (e.g., age and initial Sr isotopic ratio) for a high-Al Group B basaltic clast (,1353) from breccia 14321 (Fig. 2a). This clast, which is large enough for Rb–Sr dating, is used to test whether Group B basalts erupted at one time. This paper also reports the results of a re-evaluation of high-Al basalt eruption ages using Rb–Sr isochron ages that were obtained over a period of four decades from several different laboratories. All isotopic data were evaluated and re-processed using the same data reduction program *Isoplot 3.70* (Ludwig, 2008) and ^{87}Rb decay constant (Rotenberg et al., 2012) as used for the basaltic clast 14321,1353. With the re-calculated Rb–Sr radiometric ages, eruption episodes and petrogeneses of the high-Al basalts were then evaluated in conjunction with the ITE compositional data (where available).

2. Analytical procedures

High-Al basaltic clast sample 14321,1353 (with corresponding thin section numbers ,1355 and ,1382), which was extracted from breccia slab 14321,1310 (Fig. 2a), contains an ophitic texture dominated by plagioclase ($An_{84–95}$) and pyroxene ($En_{30–62}Fs_{24–42}$), with subordinate olivine ($Fo_{64–71}$) phenocrysts (that are reacting to pyroxene) and native iron blebs present in the mesostasis (Fig. 2b; Neal et al., 1988). Pyroxenes in this clast exhibit partial zonation from pigeonite cores to augite rims and are interstitial to plagioclase laths, which also display a zonation from An-rich cores (An >90) to more Ab-rich rims (An $\sim$85) (Neal et al., 1988). The clast is free of impact melt veining (Fig. 2b), indicating that the whole rock analysis represents that of a pristine high-Al basalt. Basaltic clast 14321,1353 was classified as a Group B high-Al basalt based on its whole-rock ITE ratios (Neal et al., 1988; Neal and Kramer, 2006).

Chips of 14321,1353 weighing $\sim$90 mg were processed for Rb–Sr isotopic analysis. No attempt was made to date the sample by the Sm–Nd isotopic system because this sample was previously irradiated for an earlier INA analysis. This irradiation has affected the Sm isotopic composition because of the neutron capture process, which requires a large correction when determining the Sm–Nd radiometric age (making such a determination very imprecise; e.g., Dasch et al., 1987; Nyquist and Shih, 1992). However, unpublished analyses of irradiated and unirradiated samples of BCR-1 in connection with the work of Dasch et al. (1987) showed no detectable effect on the Sr isotopic composition of the irradiated sample. A 20.36-mg sample was gently crushed to <100 mesh (149 μm) for the bulk rock sample (WR). Mineral separates were obtained by the heavy liquid separation on the crushed sample. Plagioclase (Plag) was mainly concentrated in the <2.85 g/cm^3 density fraction, whereas pyroxene was concentrated in the >3.32 g/cm^3 density fraction. The latter was further separated into two different density fractions: (1) 3.32–3.45 g/cm^3 Mg-rich pyroxene (Px1), and (2) >3.45 g/cm^3 Fe-rich pyroxene (Px2). The intermediate density fraction, 2.85–3.32 g/cm^3 (Plag+Px), contained intermixed plagioclase and pyroxene. Mineral separates were all washed with 1 ml of 1 N HCl and sonicated for 10 min to remove phosphates that may attach to these minerals and possible surface contamination. The acid washes of these mineral separates were combined and also analyzed ("Leach" in Table 1 and Fig. 3).

A total of six aliquots of the clast including four acid-washed mineral separates [Plag(r), Px1(r), Px2(r), and Plag+Px(r), where r=residue], one unwashed bulk rock sample (WR) and one combined leachate (Leach) were analyzed following the chemical procedures of Shih et al. (1999). The Rb and Sr isotopic measurements were made on a Finnigan-MAT 262 multi-collector mass spectrometer at NASA-Johnson Space Center following the procedures of Nyquist et al. (1994). The average values of ^{87}Sr/^{86}Sr for NBS 987 during the course of the study were 0.710275 $\pm$ 0.000033 ($2\sigma_p$, 23 analyses), normalized to ^{88}Sr/^{86}Sr=8.37521. Note σ_p is the standard deviation of the population of measurements, defined as follows: $\sigma_p = \sqrt{\sum_{i=1}^{N}(m_i-\overline{m})^2/(N-1)}$, where N is the number of measurement m_i and $\overline{m}$ is the mean value of these measurements. The ^{87}Sr/^{86}Sr results reported here were renormalized to the NBS 987 ^{87}Sr/^{86}Sr=0.710251 reported by Nyquist et al. (1990).

Table 1
The Rb–Sr analytical results for high-Al basalt clast 14321,1353.

	Wt. (mg)	Rb[b] (ppm)	Sr[b] (ppm)	^{87}Rb/^{86}Sr[c]	^{87}Sr/^{86}Sr[c,d]
<100 mesh					
WR[a]	20.36	2.88	92.8	0.0899 ± 13	0.704593 ± 10
Plag(r)[a]	6.7	2.20	215	0.0296 ± 4	0.701154 ± 13
Plag+Px(r)[a]	9.1	4.84	144	0.0974 ± 13	0.705044 ± 12
Px1(r)[a]	10.05	2.14	37.6	0.165 ± 3	0.708990 ± 10
Px2(r)[a]	2.15	1.69	22.5	0.218 ± 3	0.712216 ± 16
Leach[a]	6.1	1.04	37.3	0.0805 ± 11	0.703895 ± 13
NBS 987Sr standard:	Sr^+ (23 analyses):				0.710275 ± 33[e]

[a] WR=whole rock, Plag(r)=acid-washed plagioclase, Plag+Px(r)=acid-washed intermixed plagioclase and pyroxene; Px1(r)=acid-washed Mg-rich pyroxene, Px2(r)=acid-washed Fe-rich pyroxene, and Leach=combined acid leachates.

[b] Uncertainties of rubidium and strontium abundances are $\sim \pm 1\%$.

[c] Uncertainties correspond to last figures and represent $\pm 2\sigma_m$ error limits, where $\sigma_m = \sqrt{\sum(m_i-\overline{m})^2/(N(N-1))}$ with that N is the number of measurement m_i and that $\overline{m}$ is the mean value of these measurements.

[d] Normalized to ^{88}Sr/^{86}Sr=8.37521 and adjusted to ^{87}Sr/^{86}Sr=0.710251 of the NBS 987 Sr standard (Nyquist et al., 1990).

[e] Uncertainties correspond to last figures and represent $\pm 2\sigma_p$ error limits. See text for the definition of σ_p.

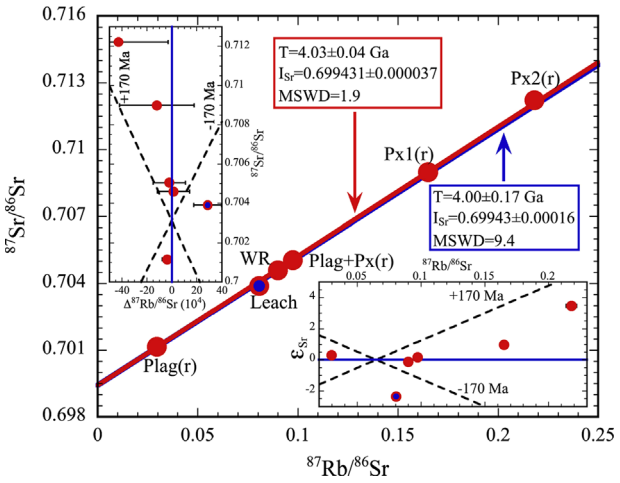

Fig. 3. Rb–Sr isochron plot for high-Al basaltic clast 14321,1353. The isochron (blue line) is calculated with all the data yields an age of 4.00 ± 0.17 Ga (blue box). If the Leach datum, which deviates from the isochron both in $^{87}Sr/^{86}Sr$ and $^{87}Rb/^{86}Sr$ ratios more than its analytical errors (as shown in the insets) is excluded, the recalculated isochron (red line) yields an age of 4.03 ± 0.04 Ga (red box). (For interpretation of the references to color in this figure legend, the reader is referred to the web version of this article.)

3. Rb–Sr age of 14321,1353

3.1. Assessment of ^{87}Rb decay constant

Precise Rb–Sr isochron age determinations require the use of an accurately and precisely determined ^{87}Rb decay constant. There are three approaches used to determine the ^{87}Rb decay constant: direct counting, age comparison, and laboratory ingrowth (Begemann et al., 2001). Many of the direct counting experiments have yielded results that are not compatible with one another within the stated uncertainties (Begemann et al., 2001). This is seen by a systematic bias between the most recent counting experiments on RbCl and $RbNO_3$, in which all measurements on $RbNO_3$ yielded higher decay constants than those on RbCl (Kossert, 2003). The accuracy of the ^{87}Rb decay constant determined using age comparison relies on two assumptions, the accurate decay constant of the other dating system (typically U–Pb) and the same closure temperature of two different age dating systems (Nebel et al., 2011), which may not actually close at the same temperature (Rotenberg et al., 2012). Among the three methods, laboratory ingrowth of ^{87}Sr is the most straightforward technique if the nuclide can accumulate for long enough to allow a precise isotopic measurement over a well-defined and extended period of time. Accumulation of ^{87}Sr in $RbClO_4$ salt used for a recent calibration of ^{87}Rb decay constant continued over three decades (Rotenberg et al., 2012), which fulfills the requirement of a well-defined and relatively long period of time. Therefore, the ^{87}Rb decay constant of 0.013968 Ga^{-1} determined from this accumulation experiment and reported in Rotenberg et al. (2012) is used in this study. Of note, the decay constant of Rotenberg et al. (2012) is similar to that of Nebel et al. (2011) and Minster et al. (1982).

3.2. Rb–Sr isochron age

The Rb and Sr concentrations and $^{87}Rb/^{86}Sr$ and $^{87}Sr/^{86}Sr$ data for whole rock, mineral separates and leachate are listed in Table 1. All six measurements form a linear array in the $^{87}Rb/^{86}Sr$ and $^{87}Sr/^{86}Sr$ isochron diagram (Fig. 3), yielding a Rb–Sr radiometric age of 4.00 ± 0.17 Ga and initial $^{87}Sr/^{86}Sr$ (I_{Sr}) of 0.69943 ± 0.00016 for $\lambda(^{87}Rb)$= 0.013968 Ga^{-1} (Rotenberg et al., 2012). The York (1969) regression algorithm was used in the program *Isoplot 3.70* (Ludwig, 2008). This Rb–Sr isochron age is within the age ranges (3.95–4.33 Ga) of other high-Al basalts and basaltic clasts reported in the literature (Papanastassiou and Wasserburg, 1971; Compston et al., 1971a, 1972; de Laeter et al., 1973; Mark et al., 1973, 1974, 1975; Dasch et al., 1987, 1991). The large scattering of data around the isochron (insets of Fig. 3), which was also observed in other Rb–Sr isotopic studies of the high-Al basalts (e.g., Dasch et al., 1987), may in part be due to isotopic disturbances caused by the impact-related thermal metamorphism during breakup of the original lava flow and formation of breccia 14321. The leachate (Leach) datum deviates from the isochron both in $^{87}Sr/^{86}Sr$ and $^{87}Rb/^{86}Sr$ ratios in excess of its associated uncertainties (insets of Fig. 3). Possible reasons may be related to the fact that dissolved phosphates and/or surface layers of the minerals are more readily disturbed during impact. Additionally the "Leach" sample combined leachates from all of the minerals from which "residues" were prepared. Thus, this aliquot is the most likely to contain any external contamination (i.e., it represents the laboratory blank, and dissolved phosphates and/or surface layers of the minerals that may be disturbed during impact) and it was analyzed as a procedural control. The results of the analysis are acknowledged to be less robust than those of the other analyses as all the other five data points fall on the isochron within their analytical errors (insets of Fig. 3). The isochron re-calculated without the leachate analysis yields a Rb–Sr isochron age of 4.03 ± 0.04 Ga and an I_{Sr} of 0.699431 ± 0.000037 (Fig. 3). This regression is more robust than that with all six data points as seen by its mean square weighted deviation (MSWD), which is significantly reduced from 9.4 to 1.9 (Fig. 3). The age of 4.03 ± 0.04 Ga is therefore interpreted to represent the crystallization age of basaltic clast 14321,1353.

4. Reassessment of literature ages

The availability of samples to produce Rb–Sr isochrons for the high-Al basalt suites is now extremely limited. However, the Rb–Sr age dating method was used the most in establishing lunar geochronology (e.g., Nyquist, 1977). Therefore, a literature review was undertaken to obtain Rb–Sr isotopic data of the high-Al basalts and basaltic clasts (Table 2).

All the literature Sr isotopic data obtained by several laboratories over the last four decades were normalized to $^{88}Sr/^{86}Sr$=8.3752 (Table 2 and references there cited). Furthermore, it has been demonstrated that the corrections for inter-laboratory bias on isotopic measurements are rather small and negligible relative to the uncertainty associated with the isochron age (Nyquist, 1977). In contrast, the calculated literature Rb–Sr isochron ages and I_{Sr} of high-Al basalts may not be directly comparable due to the use of the different ^{87}Rb decay constants (e.g., Aldrich et al., 1956; Begemann et al., 2001, and references therein), and the variable data reduction methods used by different laboratories. Therefore, it is necessary to re-process the existing literature isotopic data before any comparison can be made between the isochron ages, as well as I_{Sr}.

The published Rb–Sr isotopic data were re-processed using the program *Isoplot 3.70* (Ludwig, 2008) with $\lambda(^{87}Rb)$= 0.013968 Ga^{-1} (Rotenberg et al., 2012) following the age determination procedure for basaltic clast 14321,1353 (outlined above). To obtain a robust regression, each sample aliquot analysis was evaluated by comparing its deviation from the isochron and its associated uncertainty as demonstrated in insets of Fig. 3. Any datum that deviated from the isochron more than its associated analytical errors both in $^{87}Sr/^{86}Sr$ and $^{87}Rb/^{86}Sr$ was omitted in a second isochron regression (insets of Fig. 3). This iterative process continued until none of the remaining data deviated from the final isochron more than its analytical errors either in $^{87}Sr/^{86}Sr$ or $^{87}Rb/^{86}Sr$, which indicates a robust regression. This procedure of iterative data rejection has been previously applied to lunar samples (e.g., Dasch et al.,

Table 2
Rb-Sr isotopic data for Apollo 14 and other lunar high-Al basalts, aluminous impact melts, and highland Mg-Suite rocks.

Sample	Rb (ppm)	Sr (ppm)	$^{87}Rb/^{86}Sr$	$^{87}Sr/^{86}Sr$	Age[a] (Ga)	I_{Sr}[a]	Isochron (MSWD)	Gp[e]	Average age[a] (MSWD)	Average I_{Sr}[a] (MSWD)	Refs.
14321,9059	0.685	77.7	0.0255	0.70073	4.31 ± 17	0.699134 ± 72	0.99	A[d]	4.26 ± 10 (0.72)	0.699102 ± 47 (1.4)	Dasch et al. (1987) and Dickinson et al. (1985)
14321,1384	0.736	61.7	0.0345	0.70117	4.22 ± 13	0.699078 ± 62	1.3	A[d]			Dasch et al. (1987) and Shervais et al. (1985)
14321,1353	2.88	92.8	0.0899	0.704593	4.03 ± 4	0.699431 ± 37	1.9	B[d]	4.04 ± 6 (3.1)	0.699404 ± 64 (3.5)	This study and Neal et al. (1988)
14321,90xx[b,g]	2.83	103.6	0.0791	0.70398	4.12 ± 6	0.699387 ± 51	1.3	B[d]			Dasch et al. (1987) and Dickinson et al. (1985)
14321,9056	2.95	105.6	0.0809	0.70414	4.05 ± 6	0.699404 ± 59	0.53	B[d]			Dasch et al. (1987) and Dickinson et al. (1985)
14321,88,6A[c,g]	3.88	95.2	0.1179	0.70623	4.01 ± 4	0.699314 ± 68	1.6	B[d]			Compston et al. (1972), de Laeter et al. (1973) and Taylor et al. (1972)
14321,184–55	2.33	96.99	0.0678	0.70339	3.99 ± 14	0.69957 ± 16	0.63	B[d]			Mark et al. (1973) and Wänke et al. (1972)
14321,1394[f]	2.54	102.3	0.0719	0.70349	4.11 ± 6	0.699347 ± 55	–	B[d]	–	–	Dasch et al. (1987) and Shervais et al. (1985)
14321,478	2.93	95.97	0.0879	0.70433	–	–	–	B[d]	–	–	Mark et al. (1974) and Lindstrom et al. (1972)
14053	2.389	117.79	0.05724	0.70276	3.94 ± 3	0.699484 ± 41	1.9	C[d]	3.94 ± 3	0.699484 ± 41	Papanastassiou and Wasserburg (1971) and Neal and Kramer (2006)
14072,2[g]	1.21	81.6	0.0436	0.70183	3.98 ± 15	0.69924 ± 14	3.4	D[d]	3.98 ± 8 (0.0064)	0.699305 ± 73 (1.2)	Compston et al. (1972), de Laeter et al. (1973) and Taylor et al. (1972)
14072,48	–	–	0.04443	0.701871	3.97 ± 9	0.699330 ± 86	18	D[d]			Dasch et al. (1991) and Taylor et al. (1972)
14321,88,4A[c]	2.57	81.0	0.0918	0.70484	4.05 ± 10	0.69938 ± 15	3	HA	–	–	Compston et al. (1971a) and de Laeter et al. (1973)
14321,191-x	3.628	106.22	0.0964	0.70484	3.93 ± 6	0.699417 ± 61	0.47	HA	–	–	Papanastassiou and Wasserburg (1971)
14321,371[c,g]	2.57	108.3	0.0687	0.70317	3.97 ± 8	0.699255 ± 74	1.3	HA	–	–	Mark et al. (1975)
14321,554	2.62	103.3	0.0730	0.70340	–	–	–	HA	–	–	Mark et al. (1975)
14321,553(f)	2.46	105.9	0.0749	0.70397	–	–	–	HA	–	–	Mark et al. (1975)
14321,553(m)	1.471	59.7	0.0713	0.70335	–	–	–	HA	–	–	Mark et al. (1975)
14078,2[g]	13.73	187.8	0.2115	0.71223	3.86 ± 2	0.700508 ± 47	0.013	IM[d]	3.86 ± 1 (1.3)	0.700353 ± 76 (13)	McKay et al. (1978)
14001,7,3	22.20	263.0	0.2384	0.71360	3.87 ± 3	0.700361 ± 54	1.2	IM[d]			Papanastassiou and Wasserburg (1971)
14150,7,2	12.40	181.5	0.1977	0.71140	3.84 ± 4	0.70056 ± 14	1.18	IM[d]			McKay et al. (1979)
14150,7,3	13.71	186.2	0.2130	0.71226	3.88 ± 2	0.700371 ± 66	1.6	IM[d]			McKay et al. (1979)
14276	13.24	224.7	0.1663	0.70940	3.86 ± 2	0.700186 ± 44	0.25	IM[d]			Wasserburg and Papanastassiou (1971)
14073	15.29	205.0	0.2107	0.71200	3.86 ± 2	0.700343 ± 38	0.005	IM[d]			Papanastassiou and Wasserburg (1971)
14310	14.13	218.8	0.1824	0.71041	3.85 ± 2	0.700360 ± 46	2	IM[d]			Papanastassiou and Wasserburg (1971)
14310,118[g]	12.96	192.3	0.1983	0.71144	3.92 ± 6	0.70045 ± 14	5.5	IM[d]			Compston et al. (1972) and de Laeter et al. (1973)
14310,133	10.99	158.8	0.20039	0.71159	3.90 ± 19	0.70033 ± 62	0.093	IM[d]			Murthy et al. (1972)
14310,71	9.79	154.8	0.1832	0.71041	3.83 ± 10	0.70020 ± 23	3.2	IM[d]			Tatsumoto et al. (1972)
12031,25	0.797	153.1	0.01506	0.70020	3.22 ± 13	0.69956 ± 12	2.8	OA	–	–	Nyquist et al. (1979)
12038,22	0.587	191.4	0.00887	0.69964	3.34 ± 12	0.699216 ± 28	0.96	OA	–	–	Nyquist et al. (1981b)
12038,45	0.6	186	0.0094	0.69972	3.33 ± 20	0.699350 ± 61	1.5	OA	–	–	Compston et al. (1971a, 1971b)
L16-B1	1.855	498	0.01051	0.69965	3.39 ± 43	0.699065 ± 87	2.8	OA	–	–	Papanastassiou and Wasserburg (1972)
77215	6.177	65.46	0.2733	0.71641	4.39 ± 6	0.69902 ± 12	5.7	MS	–	–	Nakamura et al. (1976)
78236	0.862	104	0.02398	0.70057	4.36 ± 4	0.699073 ± 35	0.35	MS	–	–	Nyquist et al. (1981a)
78238	1	30.97	0.09426	0.705041	4.39 ± 2	0.699072 ± 22	2.0	MS	–	–	Edmunson et al. (2009)

[a] The Rb–Sr isotopic compositions were re-processed using *Isoplot 3.70* (Ludwig, 2008) with $\lambda(^{87}Rb)=0.013968\ Ga^{-1}$ (Rotenberg et al., 2012). The weighted average age and I_{Sr} for each group were calculated using *Isoplot 3.70* (Ludwig, 2008). Uncertainties correspond to last figures. (See text for discussion.)

[b] Average of clasts ,9065; ,9067; ,9068; ,9069; and ,9072 in breccia 14321.

[c] Whole rock composition calculated proportionally from mineral and density fractions and these whole-rock data are not included in the discussion.

[d] The sample was classified using whole-rock ITE composition.

[e] Group (Gp) represents high-Al basalt Group A, B, C or D; HA is Apollo 14 high-Al basalts which cannot be classified into Group A, B, C or D with available data; IM represents aluminous Impact Melts. See text for more explanation of Group D basalt; OA is the high-Al basalts returned by Apollo 12 and Luna 16 missions; MS means highland Mg Suite.

[f] Only two of four data points fall on the isochron within their analytical errors. Hence this sample is not included in the further discussion.

[g] Samples with data points rejected in isochron iteration compared to literature isochron calculations. 14321,90XX and 14321,371: 1 of 5 points; 14321,88,6A and 14078,2: 1 of 6 points; 14072,2: 2 of 6 points; 14310,118: 3 of 9 points were rejected.

1987). A comparison of the re-calculated ages based on the final isochron with the published ages demonstrates there were inconsistencies between isochron determinations from the different laboratories (Fig. 4). The re-calculated ages and I_{Sr} of the high-Al basalts along with their corresponding published Rb–Sr isotopic compositions are listed in Table 2. Literature Rb–Sr isotopic compositions of impact melts (Table 2) were also re-processed using the same procedure in order to compare Rb–Sr ages and I_{Sr} between these two petrogenetically different high-Al basaltic melts.

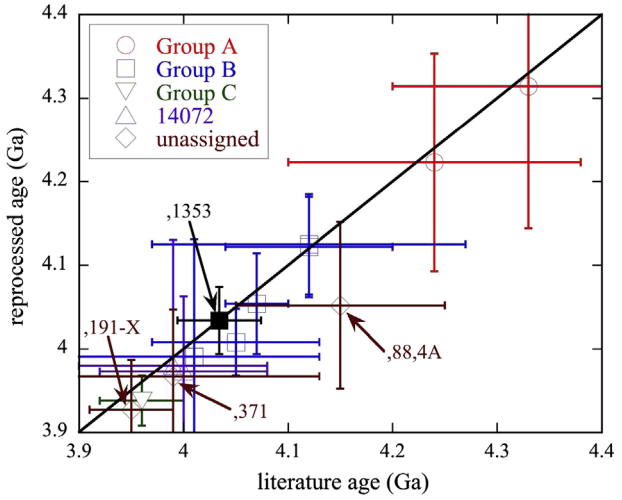

Fig. 4. A comparison of the reprocessed and published ages for Apollo 14 high-Al basalts. The data sources are listed in Table 2. The unassigned high-Al basalts and basalt, 1353 dated in this study are also clasts from breccia 14321. The reprocessed isochron ages and associated uncertainties were obtained following the procedure outlined for basalt 14321,1353 (see text for details).

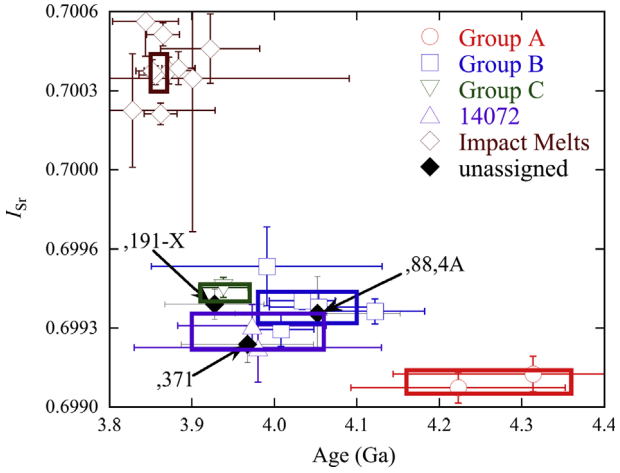

Fig. 5. I_{Sr} of Apollo 14 high-Al basalts and aluminous impact melts (obtained by the reprocessing of literature data) plotted against their corresponding reprocessed ages. The data sources are listed in Table 2. The rectangle represents the weighted-average isochron age and I_{Sr} for each group with 2σ errors. See text for discussion.

5. Discussion

5.1. Rb–Sr isotopic provenance

5.1.1. High-Al basalts: volcanic eruption episodes

Previous studies of high-Al basalts have shown that Groups A–C basalts are distinct based on ITE ratios and that basalt 14072 does not fall into any of these three groups (Neal and Kramer, 2006; Hui et al., 2011). Due to the limit of material availability, basalt 14053 is the only sample in Group C that has been dated (Table 2). In general, high-Al basalts within each group have similar crystallization ages; however, assessing the isotopic nature of their respective source regions is not possible given the overlapping 2σ uncertainties in published data (Fig. 5; Table 2). On the basis of the Rb–Sr isochron age or I_{Sr}, basalt 14072 is indistinguishable from Groups B and C basalts due to the associated large uncertainties (Fig. 5; Table 2). Basalt clasts 14321,371, 14321,88-4A, and 14321,191-x have similar Rb–Sr radiometric age and I_{Sr} values to 14072 (both subsamples—14072,2 and 14072,48), Group B, and Group C respectively. However, the isochron ages have large uncertainties and thus are not distinguishable (Fig. 5; Table 2). Furthermore, no whole-rock ITE data have been published to verify their group assignments, so for this study we treat them as "unassigned" high-Al basalts.

Since some Rb–Sr isochron ages and I_{Sr} reprocessed from the literature still have large uncertainties (Fig. 5; Table 2), new more precise Rb–Sr isotopic data for high-Al basalts are needed, which will refine the Rb–Sr isotopic provenance of each group. Nonetheless, the isochron ages of basalts in each group are overlapping within their associated uncertainties (Table 2). If it is assumed that all the high-Al basalts in each group crystallized at the same time, a weighted average age for each basalt group can be calculated with available Rb–Sr isochron ages of the high-Al basalts (Table 2). For each sample in a group, its isochron age has an uncertainty. Therefore, the age of this group can be calculated by averaging all the isochron ages weighted by the inverse-square of its isochron regression error as $\sum_{i=1}^{n}(t_i/\sigma_i^2)/\sum_{i=1}^{n}(1/\sigma_i^2)$, where t and σ stand for the isochron age and its uncertainty for the basalt, respectively. In this error-weighted average calculation, only errors from the isochron regression (Table 2) were propagated to calculate 2σ uncertainties if the probability of fit (the probability that the isochron regression errors will yield at least the amount of scatter actually observed) is more than 0.05 (Ludwig, 2008). If the probability of fit is smaller than 0.05, the error of the weighted average is the 2σ internal error multiplied by the square root of the MSWD (thus using the actual scatter of the data rather than the predicted scatter), and Student's-t test for $N-1$ degrees of freedom (to account for the fact that the true data-point errors are only an estimate, derived from the N data points) (Ludwig, 2008). A weighted average of the I_{Sr} for each basalt group was also calculated using the same method (Table 2).

Assuming the weighted average age and I_{Sr} represent the crystallization age (i.e., the magma eruption time) and source I_{Sr} of each high-Al basalt group, a plot of weighted average age versus weighted average I_{Sr} could define the isotopic provenance for the different basalt groups (Fig. 5). It is evident that our new Rb–Sr isochron age (4.03 ± 0.04 Ga) of basaltic clast 14321,1353 supports the eruption of Group B basalts at 4.04 ± 0.05 Ga, after Group A basalts (4.26 ± 0.10 Ga), but before Group C basalts (3.94 ± 0.03 Ga) (Fig. 5; Table 2). The weighted average crystallization age of basalt 14072 is 3.98 ± 0.08 Ga. This age is indistinguishable from the ages of Groups B and C basalts, as well as I_{Sr} (Fig. 5). Although the I_{Sr} for Groups B and C basalts are within error, using the weighted average values have allowed the isotopic provenance of high-Al basalts to be evaluated (Fig. 5).

5.1.2. Apollo 14 aluminous impact melts

The impact melts were initially interpreted to be primary basalts (e.g., Gancarz et al., 1971; Longhi et al., 1972; Papanastassiou and Wasserburg, 1971) until the impact origin of sample 14310 was recognized (e.g., Lofgren, 1977). Qualitative petrographic examination cannot determine whether these crystalline rocks represent a partial melt from the lunar interior or are impact-generated (e.g., Ridley et al., 1972). However, a quantitative petrographic approach using crystal size distributions (CSDs) of plagioclase appears to distinguish basaltic samples formed by melting of the lunar interior from those formed by impact melting (Hui et al., 2011; Neal et al., 2011). Additionally, the impact melts have distinct trace-element abundances compared to the high-Al basalts (e.g., Neal and Kramer, 2006; Hui et al., 2011). From this study, the impact melts also have a more radiogenic I_{Sr} and younger crystallization ages than the high-Al basalts (Fig. 5; Table 2).

The weighted average age and I_{Sr} of the impact melts are 3.86 ± 0.01 Ga and 0.700353 ± 0.000076, respectively (Fig. 5; Table 2). The trace-element distributions in plagioclase from the impact melts indicate evolution through closed-system fractional crystallization, and thus highly unlikely that the impact melts crystallized far away from the impact site (Hui et al., 2011). Therefore, it is unclear if formation of the impact melts was associated with that of the Imbrium basin (e.g., Deutsch and Stöffler, 1987) since both are of similar age (age of the Imbrium basin = 3.85 ± 0.02 Ga; e.g., Stöffler and Ryder, 2001). The relatively high I_{Sr} and trace-element abundances indicate that KREEP was one component of the mixture to form the impact melts, along with anorthosite suggested by the "high-Al" signature (Neal and Kramer, 2006; Hui et al., 2011).

5.2. Geochemical coherence within the high-Al basalt clan

The petrogenesis of the Apollo 14 high-Al basalts has been debated for decades (e.g., Ridley et al., 1972; James, 1973; Ridley, 1975; Neal et al., 1988, 1989; Neal and Taylor, 1990; Nyquist and Shih, 1992; Snyder et al., 2000; Hagerty et al., 2005; Neal and Kramer, 2006; Hui et al., 2011). It is evident that a single stage magmatic process cannot account for the geochemical diversity of the high-Al basalt suite (Fig. 6). Different Rb–Sr evolution paths may exist, corresponding to different compositional groups of high-Al basalts (Fig. 6). Furthermore, Groups B and C basalts, and basalt 14072 fall between the evolution paths of Group A basalt and KREEP material returned during the Apollo 14 mission (evolution line of $^{87}Rb/^{86}Sr = 0.242$ in Fig. 6, which is the average of four KREEP samples: 14161,35,2; 14161,35,4; 14307,26,1 and 14163,65,2; Nyquist et al., 1972). The selection criteria to calculate Apollo 14 KREEP (Fig. 6) are (1) the Rb–Sr model age is approximately 4.42 ± 0.07 Ga, which represents the model age of urKREEP formation (Nyquist and Shih, 1992; Shearer et al., 2006), with urKREEP being the hypothetical lunar magma ocean residuum (the German prefix ur-, meaning primeval; Warren and Wasson, 1979),

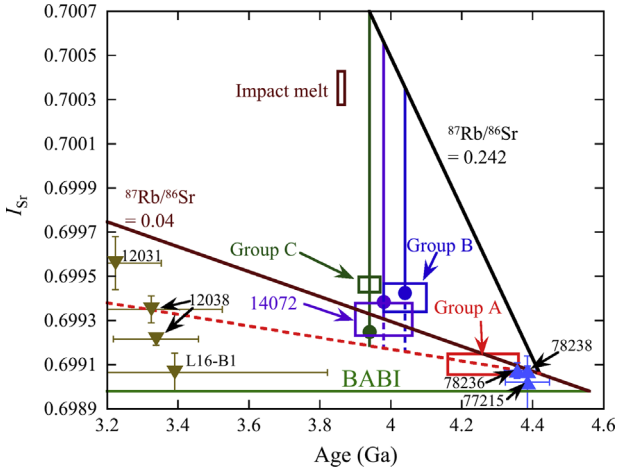

Fig. 6. Rb–Sr evolution diagram of lunar high-Al basaltic melts and the highlands Mg Suite. The solid lines are evolution paths of Basaltic Achondrite Best Initial (BABI), the Bulk Moon ($^{87}Rb/^{86}Sr \approx 0.04$; Nyquist, 1977; Neal and Taylor, 1990) and Apollo 14 KREEP ($^{87}Rb/^{86}Sr \approx 0.242$; Nyquist et al., 1972). The dashed line is the evolution path of Group A basalts. The rectangle represents the weighted-average age and I_{Sr} for each Apollo 14 basalt group with 2σ errors. The filled circles are initial Sr ratios of Groups B and C basalts and 14072 calculated as mixtures of Apollo 14 KREEP and Group A basalts constrained by incompatible trace element ratios. The age and I_{Sr} for younger Apollo 12 and Luna 16 high-Al basalts and highland Mg Suite samples (Table 2) were obtained by reprocessing literature data in the same way as was conducted for the Apollo 14 high-Al basalts. See text for discussion and Table 2 for data sources.

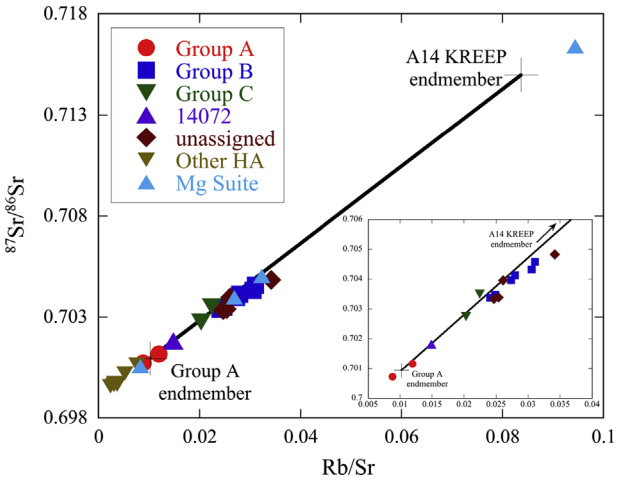

Fig. 7. Plot of $^{87}Sr/^{86}Sr$ versus Rb/Sr for high-Al basalts with mixing curves calculated between a Group A source and KREEP. The insets are focused on the Apollo 14 high-Al basalt data, which plots at the lower ends of the mixing lines. The data sources for high-Al basalts are listed in Table 2. The data for Apollo 14 KREEP are from Nyquist et al. (1972). Unassigned is for Apollo 14 high-Al basalts that have Rb–Sr isotopic data but no ITE ratio data, which means they cannot be classified using the scheme of Neal and Kramer (2006). Other HA represents Apollo 12 high-Al basalts 12031 and 12038, and Luna 16 high-Al basalt L16-B1. Mg suite is for 77215, 78236, and 78238. See text for discussion and Table 2 for data sources.

and (2) the sample is in the database for the estimation of the urKREEP composition (Warren and Wasson, 1979).

When all the high-Al basalts, regardless of the fact that they formed during different eruption episodes (Fig. 5), are evaluated together, available whole-rock Rb–Sr isotopic data generally fall on a hyperbolic mixing curve (Fig. 7; e.g., Vollmer, 1976; Langmuir et al., 1978). Two chemically and isotopically distinct end members in the mixing curves are Group A basalts and Apollo 14 KREEP. This is consistent with the fact that Groups B and C basalts, and basalt 14072 plot above this evolution trend of the Group A basalts toward that of Apollo 14 KREEP (Fig. 6).

The melt products and sources of the different high-Al basalt groups were examined using whole-rock ITE data (Neal and Kramer, 2006). The ITE ratios of the high-Al basalts of each compositional group can also be generated via mixing between the parental melt for Group A basalts (Neal and Kramer, 2006) and urKREEP (Warren and Wasson, 1979) (Fig. 8). Therefore, both Rb–Sr isotopic data and whole-rock ITE ratios indicate that parental melts of the high-Al basalts are geochemically related by progressive urKREEP addition in the order of basalt 14072, Group C, and Group B (Figs. 7 and 8). This mixing could be through two different petrogenetic processes proposed in the literature, partial melting of a hybrid mantle source (e.g., Hagerty et al., 2005), or AFC (e.g., Neal et al., 1988, 1989; Neal and Kramer, 2006).

5.3. Source regions of Apollo 14 high-Al basalts

As noted above, the Group A basalts were derived from a relatively primitive source region (i.e., a depleted mantle) in terms of incompatible trace elements and Rb–Sr isotopes, whereas the Groups B and C basalt, and basalt 14072 sources plot between the Group A basalt evolution line and that for Apollo 14 KREEP (Fig. 6). If just the parental melts of these basalt groups are examined (Neal and Kramer, 2006), they appear to be related through addition of variable amount KREEP to the Group A source (Figs. 7 and 8). Using ITE ratios that are resistant to change by partial melting and fractional crystallization (e.g., Nb/Ce), the nature of the source can be evaluated. As such, incorporation of 1.2%, 2.3%, and 11.8% of a KREEP component into the Group A source would generate the source regions for the basalt 14072, Groups C and B high-Al

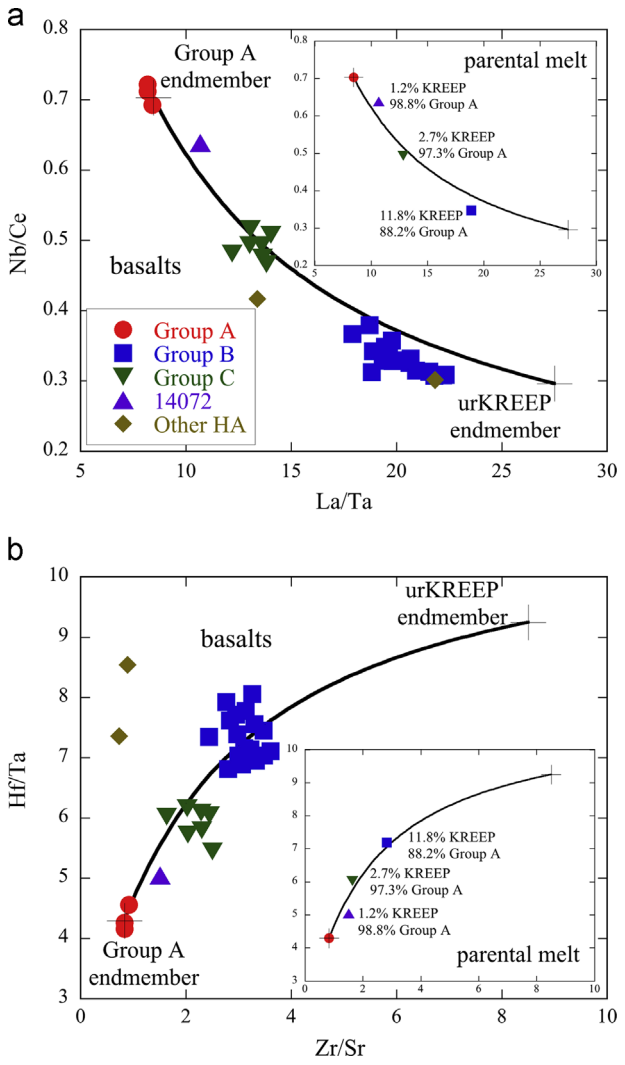

Fig. 8. ITE ratio plots for high-Al basalts with calculated mixing curves between the Group A basalt source and KREEP: (a) La/Ta versus Nb/Ce and (b) Zr/Sr versus Hf/Ta. ITE concentrations of high-Al basalts are from Neal and Kramer (2006) and those of urKREEP are from Warren and Wasson (1979). The parental melt compositions of Groups A–C basalts (shown in the insets) were derived by Neal and Kramer (2006) and that of basalt 14072 is its whole-rock composition. Note this may not represent the parental melt, but the ratios are indicative of the source region (Neal and Kramer, 2006). Other HA represents Apollo 12 high-Al basalts 12031 and 12038 (Neal, 2001).

basalts, respectively (insets of Fig. 8). This KREEP addition to the respective mantle sources is in addition to the assimilation of evolved KREEP–granite crustal components on the lunar surface (Neal and Kramer, 2006; Hui et al., 2011). Such source enrichment may have occurred through metasomatism of the lunar mantle by urKREEP components to form distinct source regions that subsequently melted to produce the different high-Al basalt groups. The scattering of whole-rock ITE ratios and Rb–Sr isotopic data around the mixing lines (Figs. 7 and 8) could be partially attributed from assimilation of evolved KREEP and/or granite crustal components (Neal and Kramer, 2006), which appears to have occurred on the lunar surface (Hui et al., 2011). This surface assimilation process during lava eruption and flow was recognized by the microdistribution of trace elements within the plagioclase grains of high-Al basalts (Hui et al., 2011). Using Sr isotopic data from Group A basalts and Apollo 14 KREEP materials, and mixing ratios constrained by ITE of parental melts, evolutions paths of Groups B and C basalts and basalt 14072 could be calculated (Fig. 6). The calculated initial isotopic ratio of Group B basalts, the most studied Apollo 14 high-Al basalt group, is consistent with the weighted average of individually analyzed basalts. However, our calculated initial Sr ratio of Group C basalts is different from that reported in the literature (Fig. 6). This may be due to the fact that only one Group C basalt (14053) has been analyzed for Rb–Sr isotopic data.

5.4. A synthesis of Apollo 14 high-Al basalt petrogenesis

The different groups of high-Al basalts experienced variable interaction with an enriched (evolved) component according to Rb–Sr isotopic compositions and ITE abundances. Analysis of the ITE ratios indicates the source regions for the different groups of high-Al basalts can be produced by variable metasomatism of a Group A basalt mantle source region by urKREEP. The Group A basalt mantle source region (relatively unadulterated by urKREEP) was depleted in terms of Rb–Sr isotopic compositions and ITE abundances (Figs. 6–8). At 4.24 ± 0.10 Ga, melting of this source region occurred, producing the parental magma of Group A basalt. Portions of a Group A-type basalt source region were variably metasomatized by urKREEP and such metasomatism may have been facilitated by the presence of volatiles in the magma ocean residuum (for example, ~1.4 wt% water in urKREEP has been inferred from indigenous OH detected in ferroan anorthosites; Hui et al., 2013). Such source regions underwent melting events at 4.04 ± 0.06 Ga to produce the Group B basalts (Group A basalt source containing 11.8% urKREEP), at 3.94 ± 0.03 Ga to produce the Group C basalts (Group A basalt source containing 2.3% urKREEP), and at 3.98 ± 0.08 Ga to produce basalt 14072 (Group A basalt source containing 1.2% urKREEP). Incorporation of ~1.2% of a KREEP component into the original Group A source would elevate the Rb/Sr ratio of the source of basalt 14072 slightly above that for the Group A basalts (Fig. 7), which would in turn allow a slightly more radiogenic $^{87}Sr/^{86}Sr$ signature to be developed over time (Fig. 6). Upon eruption of each basalt group, the lavas flowed across the surface of the Procellarum KREEP Terrane where they assimilated variable proportions of KREEP and granite (Neal and Kramer, 2006; Hui et al., 2011). Therefore, a two-stage contamination process may have occurred for the Groups B and C basalts and basalt 14072.

5.5. Relationship to other magmatic events of similar composition

Throughout the history of the Moon, there have been other high-Al magmatic events (Shearer et al., 2006, and references therein). After the formation of Apollo 14 high-Al basalts, other high-Al volcanic events occurred at ~3.3 Ga, as evidenced by the basalts 12031 (Nyquist et al., 1979), 12038 (Compston et al., 1971b; Nyquist et al., 1981b) and B-1 from Lunar 16 mission (Papanastassiou and Wasserburg, 1972) (Fig. 1a). The published Rb–Sr isotopic data for these samples have been reprocessed (Table 2) using the procedure described above. Note that 12031 and 12038 may have different petrogenetic origins from each other because the former is a member of the Pigeonite Basalt group that has accumulated plagioclase and the latter is the only representative of the Feldspathic Basalt group (Neal et al., 1994). The Luna 16 high-Al basalt has a different Rb–Sr evolution history to those from Apollo 14, as shown by that it falls below the Group A basalt evolution path (Fig. 6). Apollo 12 basalts 12038 and 12031 plot within error of the Apollo 14 Group A and Bulk Moon evolution paths, respectively, suggesting these magmas may represent a reactivation of these source regions at 3.2–3.4 Ga (Fig. 6), given the close proximity of these two Apollo sites. However, the ITE ratios demonstrate derivation from a different high-Al source compared to the Apollo 14 basalts (Figs. 7 and 8).

At the time the Apollo 14 Group A basalts erupted, the highland Mg Suite of intrusive rocks was also formed (Shearer et al., 2006). The Mg Suite rocks have similar I_{Sr} as Group A basalts (Fig. 6). Note that due to the difficulty of dating highland Mg Suites using the Rb–Sr

isotopic system, only the samples that have Rb–Sr isochron ages consistent with their Sm–Nd isochron ages were selected for comparison with this study (i.e., 77215—Nakamura et al., 1976; 78236—Nyquist et al., 1981a; 78238—Edmunson et al., 2009). As with the Apollo 12 and Luna 16 high-Al basalts, the published Rb–Sr isotopic data for these samples have also been reprocessed (Table 2) using the procedure described above to allow direct comparisons to be made. The similarity of I_{Sr} and ages (Fig. 6) suggests there may be a petrogenetic relationship between the early stages of lunar volcanism and plutonism, although the high-Al basalts have different Rb and Sr compositions compared with the Mg Suite (Fig. 7). Is it possible that the highland Mg Suite represents the plutonic equivalent of synchronous high-Al volcanism on the Moon represented by the Apollo 14 Group A basalts? Based on the lithologies in both types of samples analyzed thus far, a definitive answer to this question is not possible. The early high-Al volcanic products have been highly re-worked during the basin-forming epoch, but it may be that we have not yet sampled these outcrops and have to rely on information from breccia clasts. Kramer et al. (2008a, 2008b) suggested that high-Al basalt flows are present in Mare Imbrium, Mare Fecunditatis, Mare Nectaris, and Mare Moscoviense. Although Luna 16 returned samples from Mare Fecunditatis, none of the other areas have been directly sampled. Therefore, although the hypothesis of contemporaneous high-Al volcanism and plutonism remains to be tested, the results of this study are consistent with such a conclusion.

6. Summary

(1) On the basis of its whole-rock ITE composition (Neal et al., 1988), basaltic clast 14321,1353 is classified as a Group B high-Al basalt (Neal and Kramer, 2006) and yields a Rb–Sr isochron age of 4.03 ± 0.04 Ga and an I_{Sr} value of 0.699431 ± 0.000037, consistent with Rb–Sr determinations of other Group B high-Al basalts.

(2) Available Rb–Sr isotopic data (all reprocessed using the same procedure) and whole-rock ITE compositions for Apollo 14 high-Al basalts suggest at least three distinct Apollo 14 high-Al basalt types may be forming during different eruption episodes: 4.26 ± 0.10 Ga (Group A), 4.04 ± 0.06 Ga (Group B), and 3.94 ± 0.03 Ga (Group C). The crystallization age (3.98 ± 0.08 Ga) of basalt 14072 overlap with those of Groups B and C basalts due to large uncertainties associated with determined ages.

(3) The Rb–Sr data confirm that the high-Al basalts are distinct from impact melts (Neal and Kramer, 2006; Hui et al., 2011), which crystallized at 3.86 ± 0.01 Ga.

(4) The mantle source regions for Groups B and C high-Al basalts and basalt 14072 can be generated through variable urKREEP metasomatism of the relatively primitive mantle cumulates that formed the source for the Group A basalts. This has implications for the role of fluids within the early Moon (e.g., Hui et al., 2013), which would have facilitated such metasomatic processes.

(5) This study also reports isotopic evidence for contemporaneous high-Al volcanism and plutonism. If substantiated, this would mean widespread aluminous magmatism was occurring at least on the nearside of the Moon between 4.2 and 4.4 Ga.

Acknowledgments

This work was supported by the NASA Cosmochemistry Grant NNX09AB92G to CRN. The informal review by Tony Simonetti significantly clarified the manuscript. The constructive reviews by the editor Tim Elliott and two anonymous reviewers were invaluable in improving this paper.

Appendix A. Supplementary material

Supplementary data associated with this article can be found in the online version at http://dx.doi.org/10.1016/j.epsl.2013.04.034.

References

Aldrich, L.T., Wetherill, G.W., Tilton, G.R., Davis, G.L., 1956. Half-life of ^{87}Rb. Phys. Rev. 103, 1045–1047.
Begemann, F., Ludwig, K.R., Lugmair, G.W., Min, K., Nyquist, L.E., Patchett, P.J., Renne, P.R., Shih, C.-Y., Villa, I.M., Walker, R.J., 2001. Call for an improved set of decay constants for geochronological use. Geochim. Cosmochim. Acta 65, 111–121.
Borg, L.E., Connelly, J.N., Boyet, M., Carlson, R.W., 2011. Chronological evidence that the Moon is either young or did not have a global magma ocean. Nature 477, 70–72.
Compston, W., Vernon, M.J., Berry, H., Rudowski, R., 1971a. The age of the Fra Mauro formation: a radiometric older limit. Earth Planet. Sci. Lett. 12, 55–58.
Compston, W., Berry, H., Vernon, M.J., Chappell, B.W., Kaye, M.J., 1971b. Rubidium–strontium chronology and chemistry of lunar material from the Ocean of Storms. Proc. Lunar Sci. Conf. 2, 1471–1485.
Compston, W., Vernon, M.J., Berry, H., Rudowski, R., Gray, C.M., Ware, N., Chappell, B.W., Kaye, M., 1972. Apollo 14 mineral ages and the thermal history of the Fra Mauro formation. Proc. Lunar Sci. Conf. 3, 1487–1501.
Dasch, E.J., Shih, C.-Y., Bansal, B.M., Wiesmann, H., Nyquist, L.E., 1987. Isotopic analysis of basaltic fragments from lunar breccia 14321: chronology and petrogenesis of pre-imbrium mare volcanism. Geochim. Cosmochim. Acta 51, 3241–3254.
Dasch, E.J., Shih, C.-Y., Wiesmann, H., Bansal, B.M., Nyquist, L.E., 1991. Petrogenesis of A14 aluminous mare basalts: results from 14072,48. Proc. Lunar Planet. Sci. Conf. 22, 275–276.
de Laeter, J.R., Vernon, M.J., Compston, W., 1973. Revision of lunar Rb–Sr ages. Geochim. Cosmochim. Acta 37, 700–702.
Deutsch, A., Stöffler, D., 1987. Rb–Sr analyses of Apollo 16 melt rocks and a new age estimate for the Imbrium basin: lunar basin chronology and the early heavy bombardment of the moon. Geochim. Cosmochim. Acta 51, 1951–1964.
Dickinson, T., Taylor, G.J., Keil, K., Schmitt, R.A., Hughes, S.S., Smith, M.R., 1985. Apollo 14 aluminous mare basalts and their possible relationship to KREEP. Proc. Lunar Planet. Sci. Conf. 15, C365–C374.
Edmunson, J., Borg, L.E., Nyquist, L.E., Asmerom, Y., 2009. A combined Sm–Nd, Rb–Sr, and U–Pb isotopic study of Mg-suite norite 78238: further evidence for early differentiation of the Moon. Geochim. Cosmochim. Acta 73, 514–527.
Gancarz, A.J., Albee, A.L., Chodos, A.A., 1971. Petrologic and mineralogic investigation of some crystalline rocks returned by the Apollo 14 mission. Earth Planet. Sci. Lett. 12, 1–18.
Hagerty, J.J., Shearer, C.K., Papike, J.J., 2005. Petrogenesis of the Apollo 14 high-alumina basalts: implications from ion microprobe analyses. Geochim. Cosmochim. Acta 69, 5831–5845.
Hui, H., Oshrin, J.G., Neal, C.R., 2011. Investigation into the petrogenesis of Apollo 14 high-Al basaltic melts through crystal stratigraphy of plagioclase. Geochim. Cosmochim. Acta 75, 6439–6460.
Hui, H., Peslier, A.H., Zhang, Y., Neal, C.R., 2013. Water in lunar anorthosites and evidence for a wet early Moon. Nature Geosci. 6, 177–180.
James, O.B., 1973. Crystallization History of Lunar Feldspathic Basalt 14310. U.S. Geological Survey Professional Paper 841, 29 pp.
Kossert, K., 2003. Half-life measurements of ^{87}Rb by liquid scintillation counting. Appl. Radiat. Isot. 59, 377–382.
Kramer, G.K., Jolliff, B.L., Neal, C.R., 2008a. Distinguishing high-alumina mare basalts using Clementine UVVIS and Lunar Prospector GRS data: Mare Moscoviense and Mare Nectaris. J. Geophys. Res. 113, E01002, http://dx.doi.org/10.1029/2006JE002860.
Kramer, G.K., Jolliff, B.L., Neal, C.R., 2008b. Searching for high alumina mare basalts using Clementine UVVIS and Lunar Prospector GRS data: Mare Fecunditatis and Mare Imbrium. Icarus 198, 7–18.
Langmuir, C.H., Vocke Jr., R.D., Hanson, G.N., Hart, S.R., 1978. A general mixing equation with applications to Icelandic basalts. Earth Planet. Sci. Lett. 37, 380–392.
Lindstrom, M.M., Duncan, A.R., Fruchter, J.S., McKay, S.M., Stoeser, J.W., Goles, G.G., Lindstrom, D.J., 1972. Compositional characteristics of some Apollo 14 clastic materials. Proc. Lunar Sci. Conf. 3, 1201–1214.
Lindstrom, M.M., Haskin, L.A., 1978. Causes of compositional variations within mare basalt suites. Proc. Lunar Planet. Sci. Conf. 9, 465–486.
Lindstrom, M.M., Knapp, S.A., Shervais, J.W., Taylor, L.A., 1984. Magnesian anorthosites and associated troctolites and dunite in Apollo 14 breccias. Proc. Lunar Planet. Sci. Conf. 15, C41–C49.
Lofgren, G.E., 1977. Dynamic crystallization experiments bearing on the origin of textures in impact-generated liquids. Proc. Lunar Sci. Conf. 8, 2079–2095.

Longhi, J., Walker, D., Hays, J.F., 1972. Petrography and crystallization history of basalts 14310 and 14072. Proc. Lunar Sci. Conf. 3, 131–139.
Ludwig, K.R., 2008. Isoplot 3.70: A Geochronological Toolkit for Microsoft *Excel*. Berkeley Geochronological Center, Special Publication 4.
Mark, R.K., Cliff, R.A., Lee-Hu, C., Wetherill, G.W., 1973. Rb–Sr studies of lunar breccias and soils. Proc. Lunar Sci. Conf. 4, 1785–1795.
Mark, R.K., Lee-Hu, C., Wetherill, G.W., 1974. Equilibration and ages: Rb–Sr studies of breccias 14321 and 15265. Proc. Lunar Conf. 5, 1477–1485.
Mark, R.K., Lee-Hu, C., Wetherill, G.W., 1975. More on Rb–Sr in lunar breccia 14321. Proc. Lunar Sci. Conf. 6, 1501–1507.
McKay, G.A., Wiesmann, H., Bansal, B.M., Shih, C.-Y., 1979. Petrology, chemistry, and chronology of Apollo 14 KREEP basalts. Proc. Lunar Planet. Sci. Conf. 10, 181–205.
McKay, G.A., Wiesmann, H., Nyquist, L.E., Wooden, J.L., Bansal, B.M., 1978. Petrology, chemistry, and chronology of 14078: chemical constraints on the origin of KREEP. Proc. Lunar Planet. Sci. Conf. 9, 661–687.
Minster, J.-F., Birck, J.-L., Allègre, C.J., 1982. Absolute age of formation of chondrites studied by the ^{87}Rb–^{87}Sr method. Nature 300, 414–419.
Murthy, V.R., Evensen, N.M., Jahn, B.-M., Coscio Jr., M.R., 1972. Apollo 14 and 15 samples: Rb–Sr ages, trace elements, and lunar evolution. Proc. Lunar Sci. Conf. 3, 1503–1514.
Nakamura, N., Tatsumoto, M., Nunes, P.D., Unruh, D.M., Schwab, A.P., Wildeman, T.R., 1976. 4.4 b.y.-old clast in Boulder 7, Apollo 17: a comprehensive chronological study by U–Pb, Rb–Sr and Sm–Nd methods. Proc. Lunar Sci. Conf. 7, 2309–2333.
Neal, C.R., 2001. Interior of the Moon: the presence of garnet in the primitive deep lunar mantle. J. Geophys. Res. 106, 27865–27885.
Neal, C.R., Donohue, P., Fagan, A., Hui, H., O'Sullivan, K., 2011. Using quantitative petrography to distinguish between pristine basalts and impact melts from the Moon. In: Proceedings of the Lunar and Planetary Science Conference, vol. 42. Houston TX, Abstract # 2668.
Neal, C.R., Hacker, M.D., Snyder, G.A., Taylor, L.A., Liu, Y.-G., Schmitt, R.A., 1994. Basalt generation at the Apollo 12 site, Part 1: new data, classification, and re-evaluation. Meteoritics 29, 334–348.
Neal, C.R., Kramer, G.Y., 2006. The petrogenesis of the Apollo 14 high-Al mare basalts. Am. Mineral. 91, 1521–1535.
Neal, C.R., Taylor, L.A., 1989. Metasomatic products of the lunar magma ocean: the role of KREEP dissemination. Geochim. Cosmochim. Acta 53, 529–541.
Neal, C.R., Taylor, L.A., 1990. Modeling of lunar basalt petrogenesis: Sr isotope evidence from Apollo 14 high-alumina basalts. Proc. Lunar Planet. Sci. Conf. 20, 101–108.
Neal, C.R., Taylor, L.A., 1992. Petrogenesis of mare basalts: a record of lunar volcanism. Geochim. Cosmochim. Acta 56, 2177–2211.
Neal, C.R., Taylor, L.A., Lindstrom, M.M., 1988. Apollo 14 mare basalt petrogenesis: assimilation of KREEP-like components by a fractionating magma. Proc. Lunar Planet. Sci. Conf. 18, 139–153.
Neal, C.R., Taylor, L.A., Schmitt, R.A., Hughes, S.S., Lindstrom, M.M., 1989. High alumina (HA) and very high potassium (VHK) basalt clasts from Apollo 14 breccias, part 2—whole rock geochemistry: further evidence for combined assimilation and fractional crystallization within the lunar crust. Proc. Lunar Planet. Sci. Conf. 19, 147–161.
Nebel, O., Scherer, E.E., Mezger, K., 2011. Evaluation of the ^{87}Rb decay constant by age comparison against the U–Pb system. Earth Planet. Sci. Lett. 301, 1–8.
Nyquist, L.E., 1977. Lunar Rb–Sr chronology. Phys. Chem. Earth 10, 103–142.
Nyquist, L.E., Bansal, B., Wiesmann, H., Shih, C.-Y., 1994. Neodymium, strontium and chromium isotopic studies of the LEW86010 and Angra dos Reis meteorites and the chronology of the angrite parent body. Meteoritics 29, 872–885.
Nyquist, L.E., Bogard, D.D., Wiesmann, H., Bansal, B.M., Shih, C.-Y., Morris, R.M., 1990. Age of a eucrite clast from the Bholghati howardite. Geochim. Cosmochim. Acta 54, 2195–2206.
Nyquist, L.E., Hubbard, N.J., Gast, P.W., Church, S.E., Bansal, B.M., Wiesmann, H., 1972. Rb–Sr systematics for chemically defined Apollo 14 breccias. Proc. Lunar Sci. Conf. 3, 1515–1530.
Nyquist, L.E., Reimold, W.U., Bogard, D.D., Wooden, J.L., Bansal, B.M., Wiesmann, H., Shih, C.-Y., 1981a. A comparative Rb–Sr, Sm–Nd, and K–Ar study of shocked norite 78236: evidence of slow cooling in the lunar crust. Proc. Lunar Planet. Sci. Conf. 12B, 67–97.
Nyquist, L.E., Shih, C.-Y., 1992. The isotopic record of lunar volcanism. Geochim. Cosmochim. Acta 56, 2213–2234.
Nyquist, L.E., Shih, C.-Y., Wooden, J.L., Bansal, B.M., Wiesmann, H., 1979. The Sr and Nd isotopic record of Apollo 12 basalts: implications for lunar geochemical evolution. Proc. Lunar Sci. Conf. 10, 77–114.
Nyquist, L.E., Wooden, J.L., Shih, C.-Y., Wiesmann, H., Bansal, B.M., 1981b. Isotopic and REE studies of lunar basalt 12038: implications for petrogenesis of aluminous mare basalts. Earth Planet. Sci. Lett. 55, 335–355.
Papanastassiou, D.A., Wasserburg, G.J., 1971. Rb–Sr ages of igneous rocks from the Apollo 14 mission and the age of the Fra Mauro formation. Earth Planet. Sci. Lett. 12, 36–48.
Papanastassiou, D.A., Wasserburg, G.J., 1972. Rb–Sr of a Luna 16 basalt and the model age of lunar soils. Earth Planet. Sci. Lett. 13, 368–374.
Ridley, W.I., 1975. On high-alumina mare basalts. Proc. Lunar Sci. Conf. 6, 131–145.
Ridley, W.I., Brett, R., Williams, R.J., Takeda, H., Brown, R.W., 1972. Petrology of Fra Mauro basalt 14310. Proc. Lunar Sci. Conf. 3, 159–170.
Rotenberg, E., Davis, D.W., Amelin, Y., Ghosh, S., Bergquist, B.A., 2012. Determination of the decay-constant of ^{87}Rb by laboratory accumulation of ^{87}Rb. Geochim. Cosmochim. Acta 85, 41–57.
Ryder, G., 1976. Lunar sample 15405: remnant of a KREEP basalt–granite differentiated pluton. Earth Planet. Sci. Lett. 29, 255–268.
Shearer, C.K., Hess, P.C., Wieczorek, M.A., Pritchard, M.E., Parmentier, E.M., Borg, L. E., Longhi, J., Elkins-Tanton, L.T., Neal, C.R., Antonenko, I., Canup, R.M., Halliday, A.N., Grove, T.L., Hager, B.H., Lee, D.-C., Wiechert, U., 2006. Thermal and magmatic evolution of the Moon. Rev. Mineral. Geochem. 60, 365–518.
Shervais, J.W., Taylor, L.A., Lindstrom, M.M., 1985. Apollo 14 mare basalts: petrology and geochemistry of clasts from consortium breccia 14321. Proc. Lunar Planet. Sci. Conf. 15, C375–C395.
Shih, C.-Y., Nyquist, L.E., Wiesmann, H., 1999. Samarium–neodymium and rubidium–strontium systematics of nakhlite Governador Valadares. Meteorit. Planet. Sci. 34, 647–655.
Snyder, G.A., Borg, L.E., Nyquist, L.E., Taylor, L.A., 2000. Chronology and isotopic constrains on lunar evolution. In: Canup, R.M., Righter, K. (Eds.), Origin of the Earth and Moon. University of Arizona Press, Tucson, pp. 361–395.
Stöffler, D., Ryder, G., 2001. Stratigraphy and isotope ages of lunar geologic units: chronological standard for the inner solar system. Space Sci. Rev. 96, 9–54.
Swann, G.A., Bailey, N.G., Batson, R.M., Eggleton, R.E., Hait, M.H., Holt, H.E., Larson, K.B., Reed, V.S., Schaber, G.G., Sutton, R.L., Trask, N.J., Ulrich, G.E., Wilshire, H.G., 1977. Geology of the Apollo 14 Landing Site in the Fra Mauro Highlands. U.S. Geology Survey Professional Paper 880. 103 pp.
Tatsumoto, M., Hedge, C.E., Doe, B.R., Unruh, D.M., 1972. U–Th–Pb and Rb–Sr measurements on some Apollo 14 lunar samples. Proc. Lunar Sci. Conf. 3, 1531–1555.
Taylor, L.A., Patchen, A., Mayne, R.G., Taylor, D.-H., 2004. The most reduced rock from the moon, Apollo 14 basalt 14053: its unique features and their origin. Am. Mineral. 89, 1617–1624.
Taylor, S.R., Kaye, M., Muir, P., Nance, W., Rudowski, R., Ware, N., 1972. Composition of the lunar uplands: chemistry of Apollo 14 samples from Fra Mauro. Proc. Lunar Sci. Conf. 3, 1231–1249.
Vollmer, R., 1976. Rb–Sr and U–Th–Pb systematics of alkaline rocks: the alkaline rocks from Italy. Geochim. Cosmochim. Acta 40, 283–295.
Wänke, H., Baddenhausen, H., Balacescu, A., Teschke, F., Spettel, B., Dreibus, G., Palme, H., Quuano-Rico, M., Kruse, H., Wlotzka, F., Begemann, F., 1972. Multi-element analyses of lunar samples and some implications of the results. Proc. Lunar Sci. Conf. 3, 1251–1268.
Warren, P.H., Kallemeyn, G.W., Kyte, F.T., 1997. Siderophile element evidence indicates that Apollo 14 high-Al mare basalts are not impact melts. Lunar Planet. Sci. XXVIII, 1501–1502.
Warren, P.H., Taylor, G.J., Keil, K., Kallemeyn, G.W., Shirley, D.N., Wasson, J.T., 1983a. Seventh foray: whitlockite-rich lithologies, a diopside-bearing troctolitic anorthosite, ferroan anorthosites, and KREEP. Proc. Lunar Planet. Sci. Conf. 14, B151–B164.
Warren, P.H., Taylor, G.J., Keil, K., Shirley, D.N., Wasson, J.T., 1983b. Petrology and chemistry of two "large" granite clasts from the Moon. Earth Planet. Sci. Lett. 64, 175–185.
Warren, P.H., Wasson, J.T., 1979. The origin of KREEP. Rev. Geophys. Space Phys. 17, 73–88.
Wasserburg, G.J., Papanastassiou, D.A., 1971. Age of an Apollo 15 mare basalt: lunar crust and mantle evolution. Earth Planet. Sci. Lett. 13, 97–104.
York, D., 1969. Least squares fitting of a straight line with correlated errors. Earth Planet. Sci. Lett. 5, 320–324.